Electronic Supporting Information for

Complexes of Eu(III)$(hfa)_3$ with a planar chiral P(III) ligand (Phanephos): solvent-sensitive sign inversion of circularly polarised luminescence

Yuki Kono,[a] Nobuyuki Hara,[a] Motohiro Shizuma,[b] Michiya Fujiki[c*] and Yoshitane Imai[a*]

[a] Department of Applied Chemistry, Faculty of Science and Engineering, Kindai University, 3-4-1 Kowakae, Higashi-Osaka, Osaka 577-8502, Japan.; E-mail: (Y.I.) y-imai@apch.kindai.ac.jp.
[b] Department of Biochemistry, Osaka Municipal Technical Research Institute, 1-6-50 Morinomiya, Joto-ku, Osaka 536-8553, Japan.
[c] Graduate School of Materials Science, Nara Institute of Science and Technology, Takayama, Ikoma, Nara 630-0192, Japan. (M.F.) fujikim@ms.naist.jp.

Table of Contents

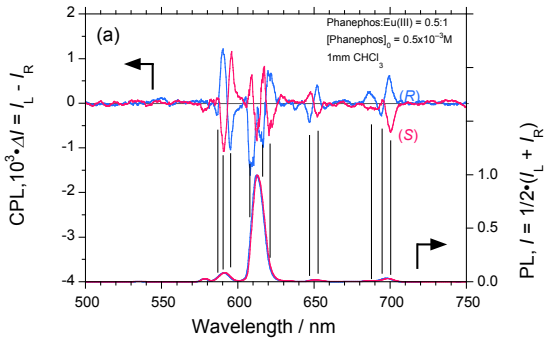

Fig. S1a. (*R*)-/(*S*)-Phanephos:Eu(hfa)$_3$ =0.5:1.

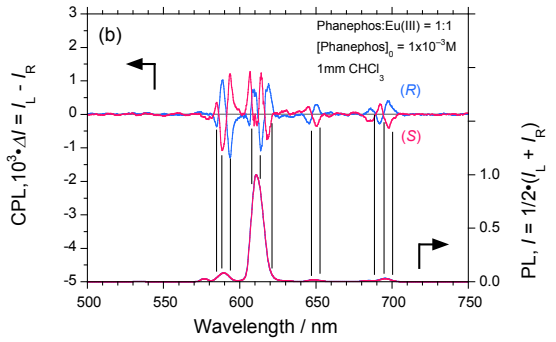

Fig. S1b. (*R*)- and (*S*)-Phanephos:Eu(hfa)$_3$ = 1:1.

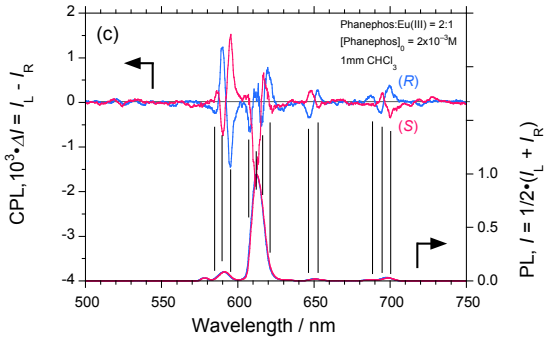

Fig. S1c. (*R*)- and (*S*)-Phanephos:Eu(hfa)$_3$ = 2:1.

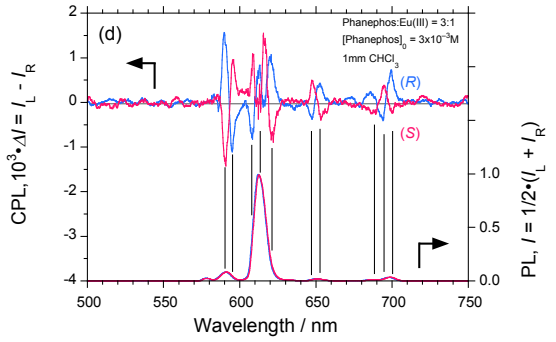

Fig. S1d. (*R*)- and (*S*)-Phanephos:Eu(hfa)$_3$ = 3:1.

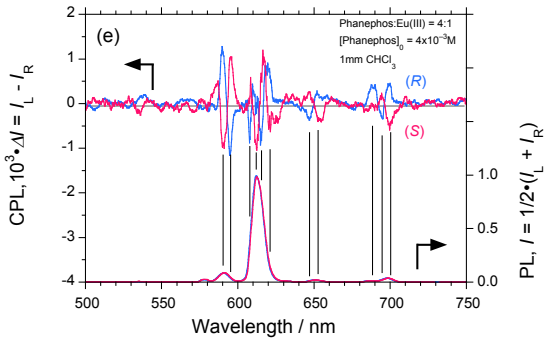

Fig. S1e. (*R*)- and (*S*)-Phanephos:Eu(hfa)$_3$ = 4:1.

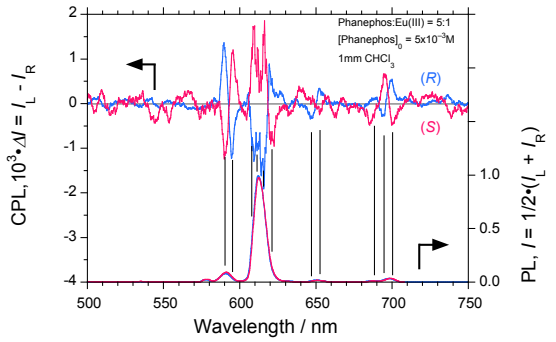

Fig. S1f. (*R*)- and (*S*)-Phanephos:Eu(hfa)$_3$ = 5:1.

Fig. S1. CPL and PL spectra as a function of (*R*)- and (*S*)-Phanephos : Eu(hfa)$_3$ ratio in EtOH-free chloroform. Path length 1.0 mm. λ_{ex} = 320 nm. [Eu(hfa)$_3$]$_0$ = 1.0 × 10^{-3} M. Bandwidth for emission 2 nm, bandwidth for excitation 16 nm, response time of PMT 16 sec, scanning rate 20 nm per min, and one scan.

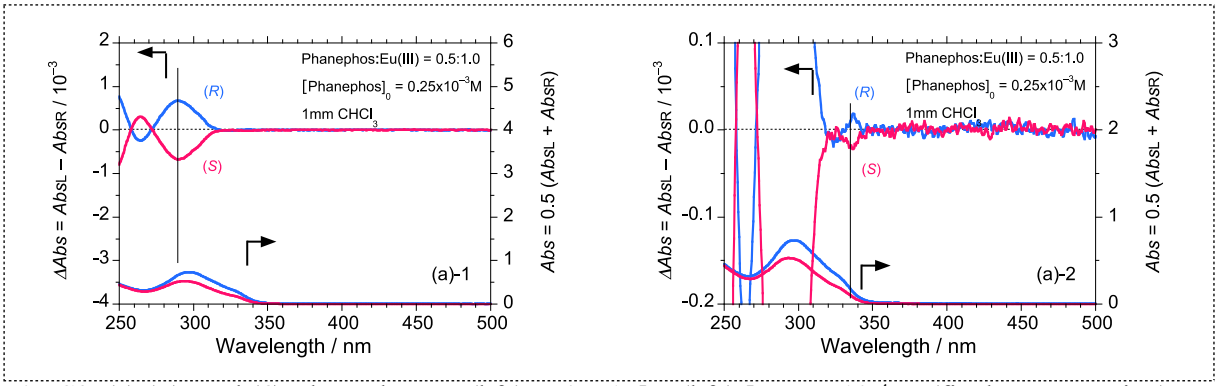

Fig. S2. (a) (*R*)- and (*S*)-Phanephos: Eu(hfa)$_3$ = 0.5:1. [Eu(hfa)$_3$]$_0$ = 5 x 10^{-4} M (final concentration), path length 1 mm.

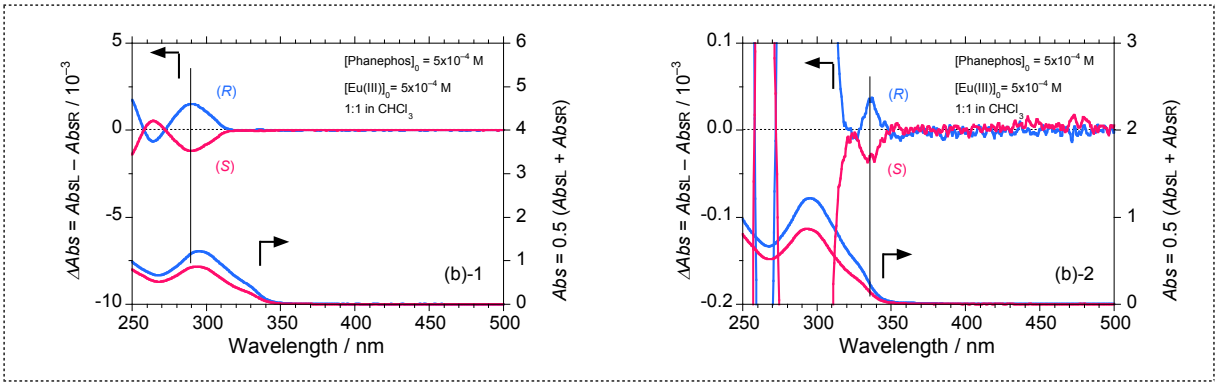

Fig. S2. (b) (*R*)- and (*S*)-Phanephos:Eu(hfa)$_3$ = 1:1. [Eu(hfa)$_3$]$_0$ = 5 x 10^{-4} M (final concentration), path length 1 mm.

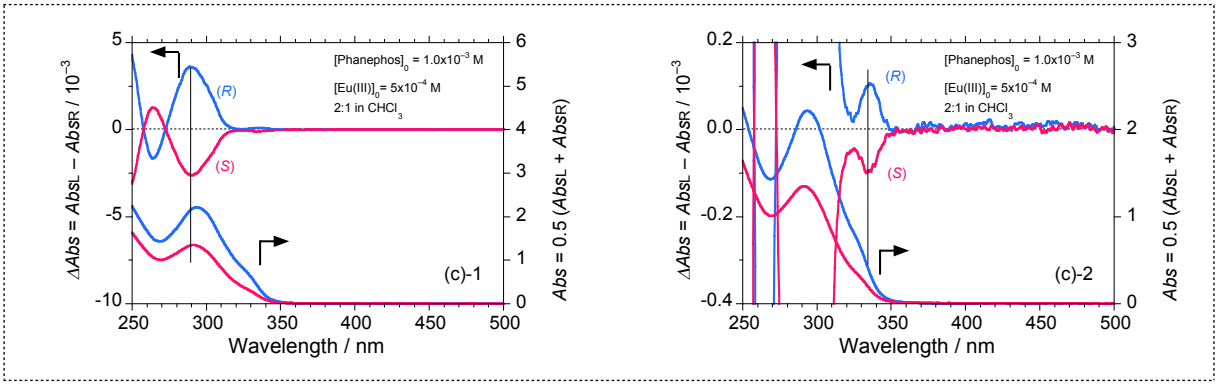

Fig. S2. (c) (*R*)- and (*S*)-Phanephos:Eu(hfa)$_3$ = 2:1. [Eu(hfa)$_3$]$_0$ = 5 x 10^{-4} M (final concentration), path length 1 mm.

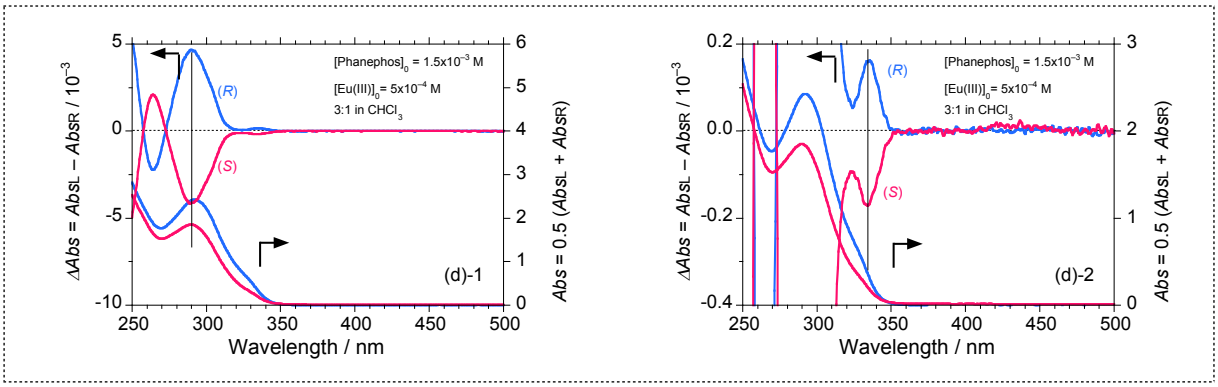

Fig. S2. (d) (*R*)- and (*S*)-Phanephos:Eu(hfa)$_3$ = 3:1. [Eu(hfa)$_3$]$_0$ = 5 x 10^{-4} M (final concentration), path length 1 mm.

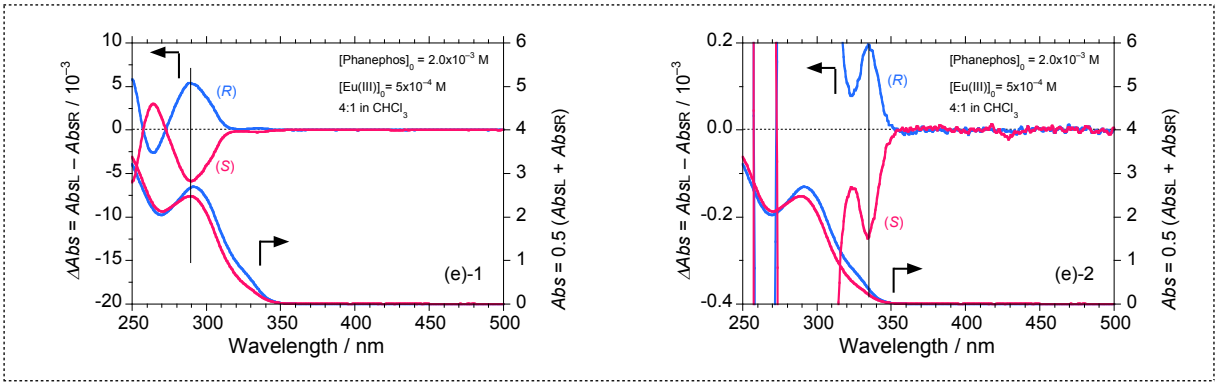

Fig. S2. (e) (*R*)- and (*S*)-Phanephos:Eu(hfa)$_3$ = 4:1. [Eu(hfa)$_3$]$_0$ = 5 x 10^{-4} M (final concentration), path length 1 mm.

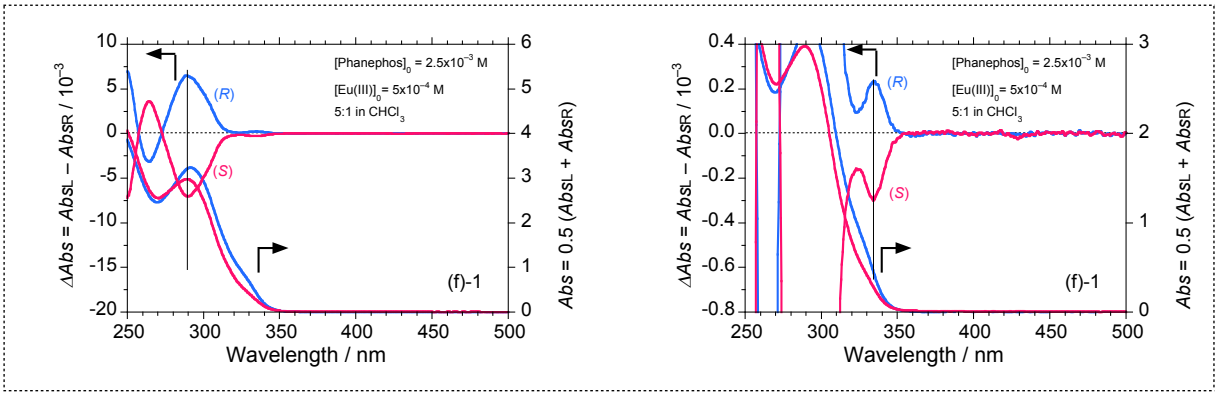

Fig. S2. (f) (*R*)- and (*S*)-Phanephos: Eu(hfa)$_3$ = 5:1. [Eu(hfa)$_3$]$_0$ = 5 x 10^{-4} M (final concentration), path length 1 mm.

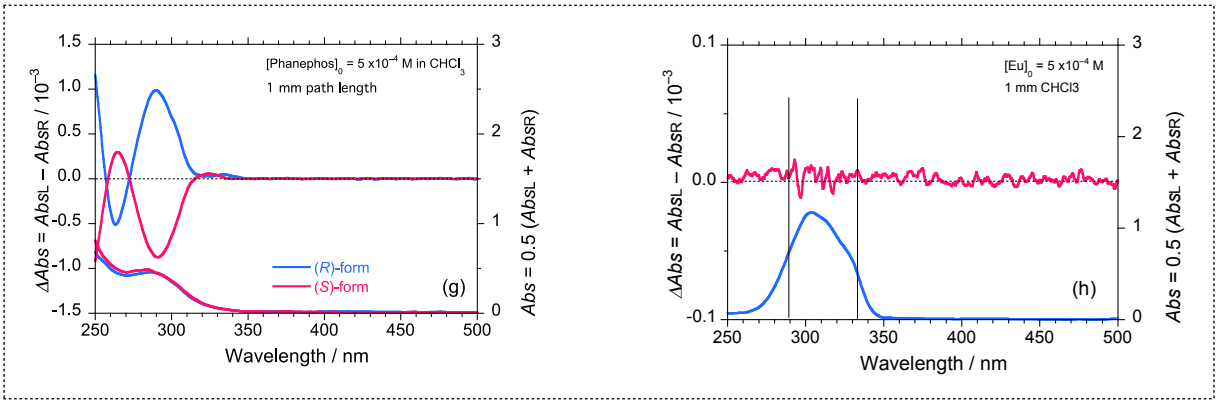

Fig. S2. (g) (*R*)- and (*S*)-Phanephos in the absence of Eu(hfa)$_3$ in $CHCl_3$. [Phanephos]$_0$ = 5 x 10^{-4} M (final concentration), path length 1 mm. (h) Eu(hfa)$_3$ in the absence of Phanephos. [Eu(hfa)$_3$]$_0$ = 5 x 10^{-4} M (final concentration), path length 1 mm.

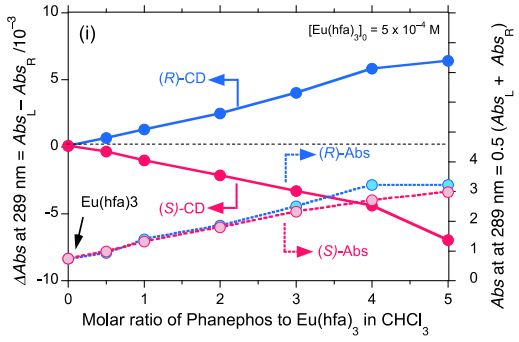

Fig. S2. (i) The CD amplitudes at 289 nm (*ΔAbs*) (left ordinate) and UV absorbance (*Abs,* right ordinate) as a function of Phanphos-to-Eu molar ratio. All data were taken from Fig. S2a–S2g.

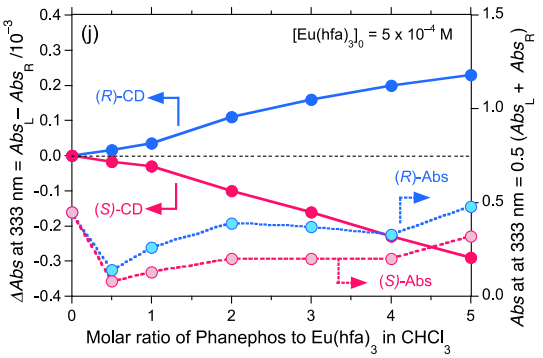

Fig. S2. (j) The CD amplitudes at 333 nm (*ΔAbs*) (left ordinate) and UV absorbance (*Abs,* right ordinate) as a function of Phanphos-to-Eu molar ratio. All data were taken from Fig. S2a–S2g.

Fig. S2. CD and UV-vis spectra of (*R*)- and (*S*)-Phanephos : $Eu(hfa)_3$ in EtOH-free chloroform. $[Eu(hfa)_3]_0 = 5 \times 10^{-4}$ M (final concentration, fixed, path length 1 mm.).

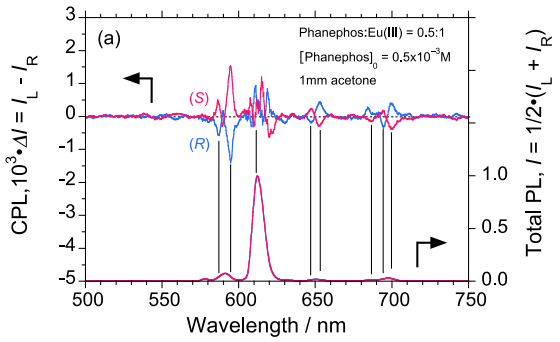

Fig. S3a. CPL and PL spectra of (*R*)- and (*S*)-Phanephos: $Eu(hfa)_3$ = 0.5:1 in acetone.

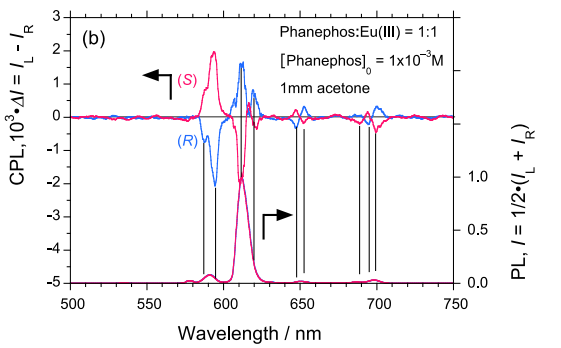

Fig. S3b. CPL and PL spectra of (*R*)- and (*S*)-Phanephos: $Eu(hfa)_3$ = 1:1 in acetone.

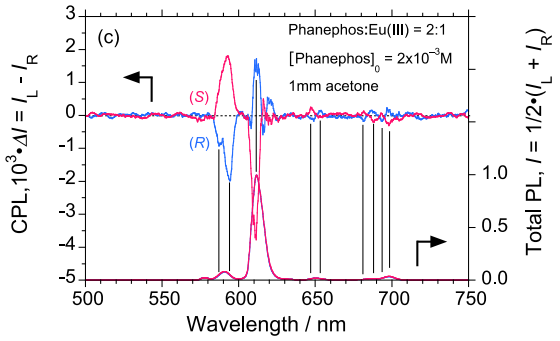

Fig. S3c. CPL and PL spectra of (*R*)- and (*S*)-Phanephos:$Eu(hfa)_3$ = 2:1 in acetone.

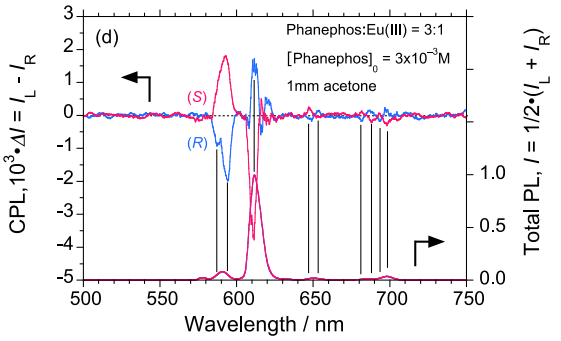

Fig. S3d. CPL and PL spectra of (*R*)- and (*S*)-Phanephos:$Eu(hfa)_3$ = 3:1 in acetone.

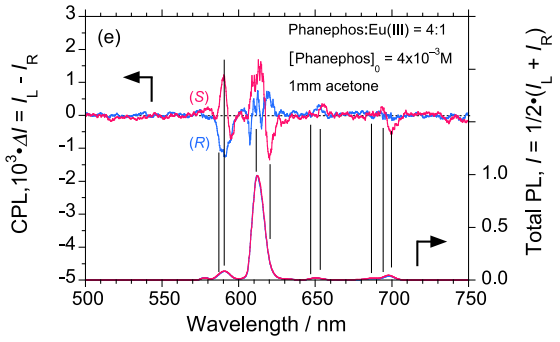

Fig. S3e. CPL and PL spectra of (*R*)- and (*S*)-Phanephos:$Eu(hfa)_3$ = 4:1 in acetone.

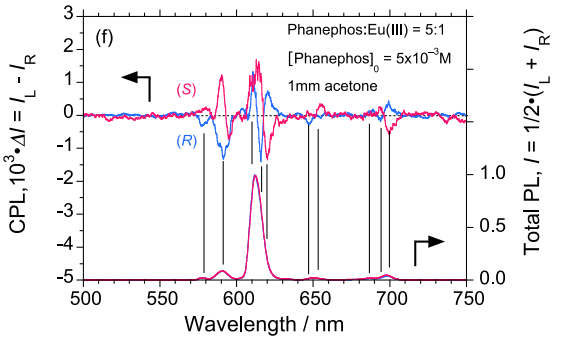

Fig. S3f. CPL and PL spectra of (*R*)- and (*S*)-Phanephos:$Eu(hfa)_3$ = 5:1 in acetone.

Fig. S3. CPL and PL spectra as a function of (*R*)- and (*S*)-Phanephos : $Eu(hfa)_3$ ratio in acetone. Path length 1.0 mm. λ_{ex} = 320 nm. $[Eu(hfa)_3]_0 = 1.0 \times 10^{-3}$ M. Bandwidth for emission 2 nm, bandwidth for excitation 16 nm, response time of PMT 16 sec, scanning rate 20 nm per min, and one-time scan.

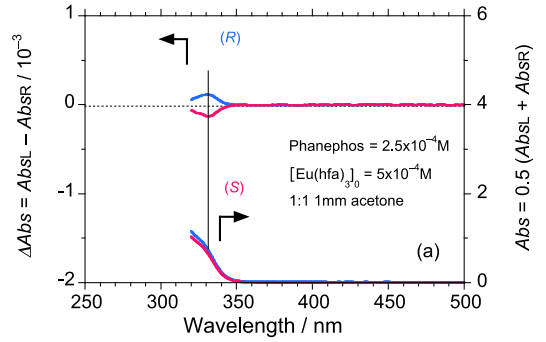

Fig. S4a. (*R*)- and (*S*)-Phanephos:Eu(hfa)$_3$= 0.5:1.

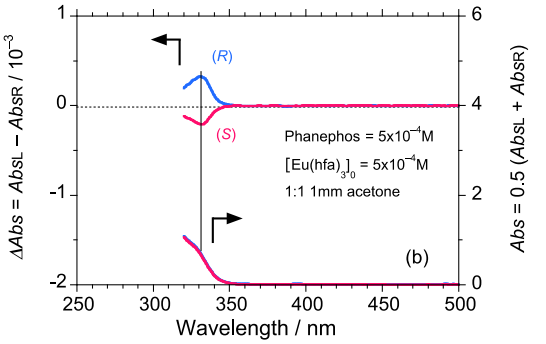

Fig. S4b. (*R*)- and (*S*)-Phanephos:Eu(hfa)$_3$ = 1:1.

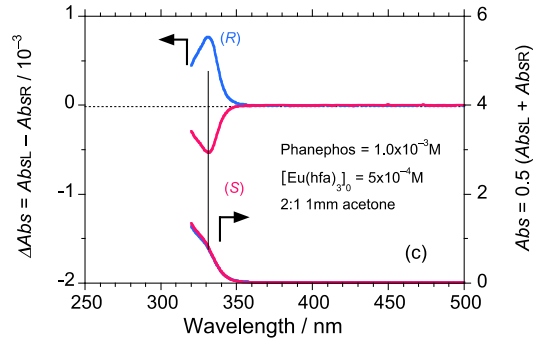

Fig. S4c. (*R*)- and (*S*)-Phanephos:Eu(hfa)$_3$= 2:1.

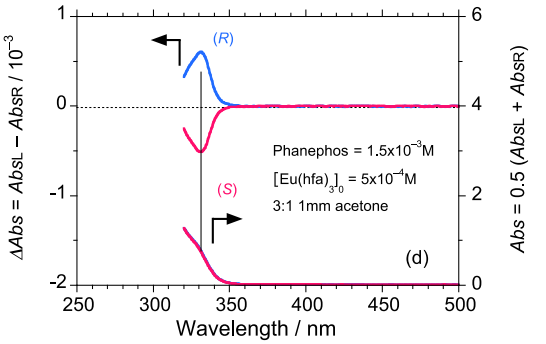

Fig. S4d. (*R*)- and (*S*)- Phanephos:Eu(hfa)$_3$= 3:1.

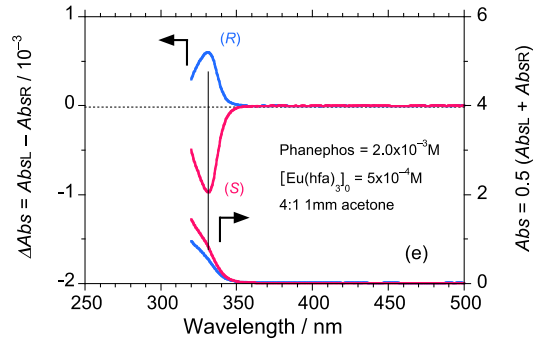

Fig. S4e. (*R*)- and (*S*)-Phanephos:Eu(hfa)$_3$=4:1.

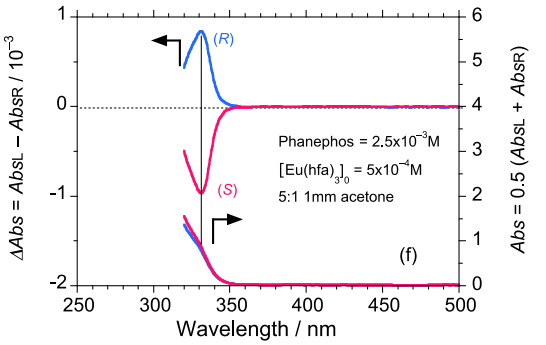

Fig. S4f. (*R*)- and (*S*)-Phanephos: Eu(hfa)$_3$=5:1.

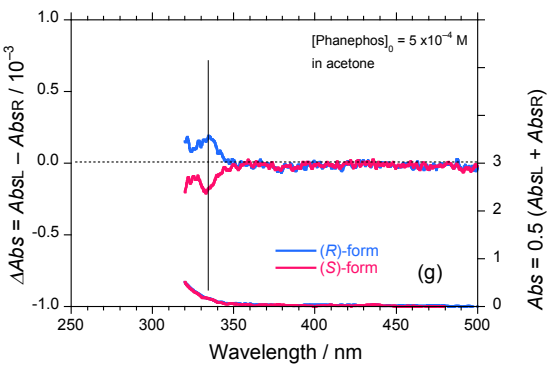

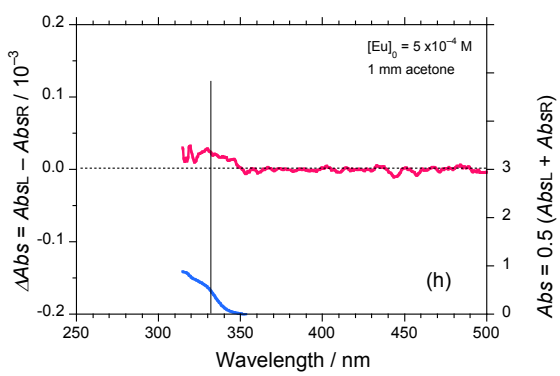

Fig. S4g. (*R*)- and (*S*)-Phanephos in the absence of Eu(hfa)$_3$ in acetone. [Phanephos]$_0$ = 5 x 10^{-4} M (final concentration), path length 1 mm.

Fig. S4h. Eu(hfa)$_3$ in the absence of Phanephos in acetone. [Eu(hfa)$_3$]$_0$ = 5 x 10^{-4} M (final concentration), path length 1 mm.

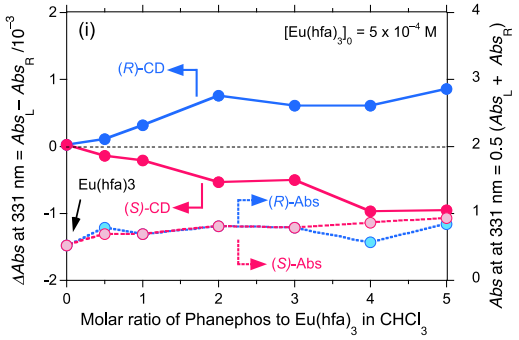

Fig. S4i. The CD amplitudes at 331 nm (*ΔAbs*) (left ordinate) and UV absorbance at 331 nm (*Abs,* right ordinate) as a function of Phanphos-to-Eu molar ratio.

Fig. S4. CD and UV-vis spectra of (*R*)- and (*S*)-Phanephos:$Eu(hfa)_3$ in acetone. $[Eu(hfa)_3]_0 = 5 \times 10^{-4}$ M (final concentration (fixed), path length 1.0 mm). UV-vis/CD spectra shorter than 320 nm are not valid because of cut-off wavelength from strong *n*-π* band of solvent acetone.

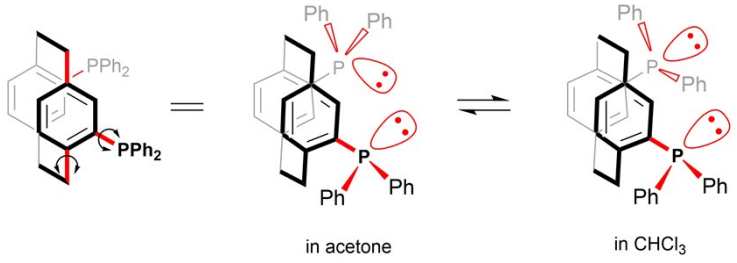

In the ground state or photoexcited state

Fig. S5. Proposed models of change in local conformation of (*R*)-Phanephos. A prefer conformation is dependent of the nature of solvent molecules in the ground and/or photoexcited states.

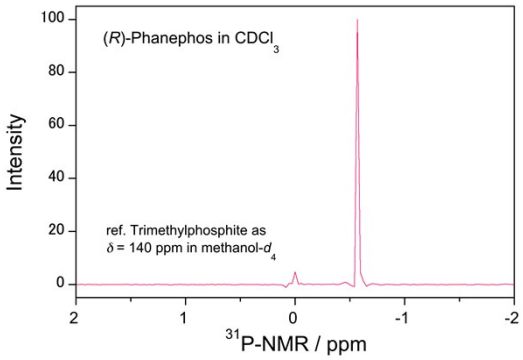

Fig. S6-a. (*R*)-Phanephos : $Eu(hfa)_3$ (1:0).

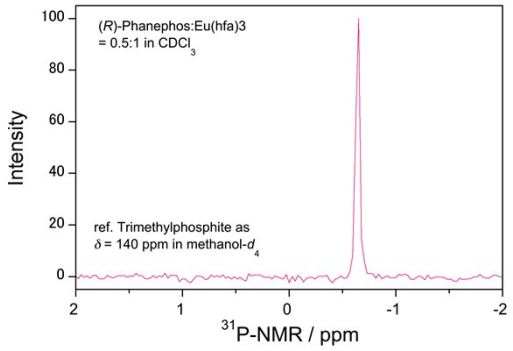

Fig. S6-b. (*R*)-Phanephos : $Eu(hfa)_3$ (0.5:1).

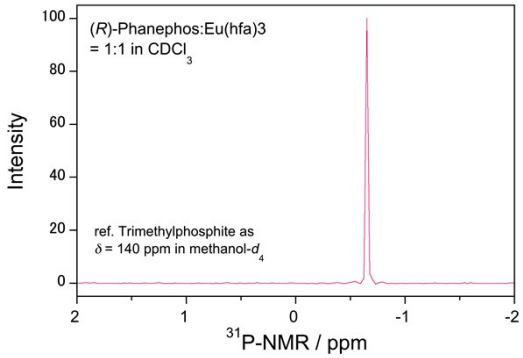

Fig. S6-c. (*R*)-Phanephos : $Eu(hfa)_3$ (1:1).

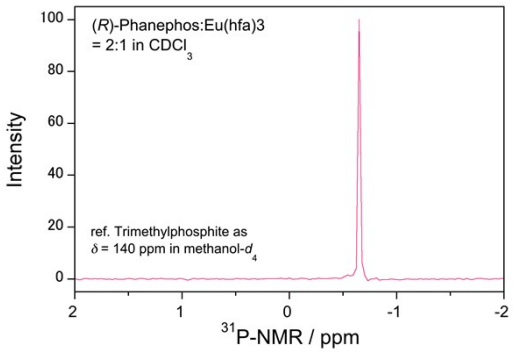

Fig. S6-d. (*R*)-Phanephos : $Eu(hfa)_3$ (2:1).

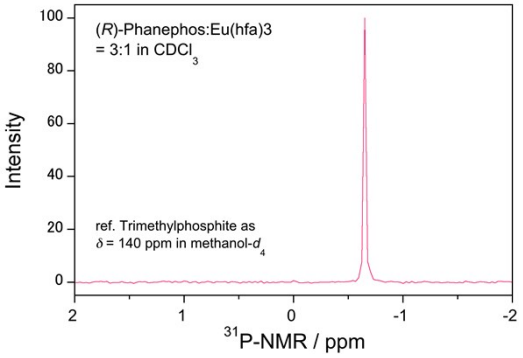

Fig. S6-e. (*R*)-Phanephos : $Eu(hfa)_3$ (3:1).

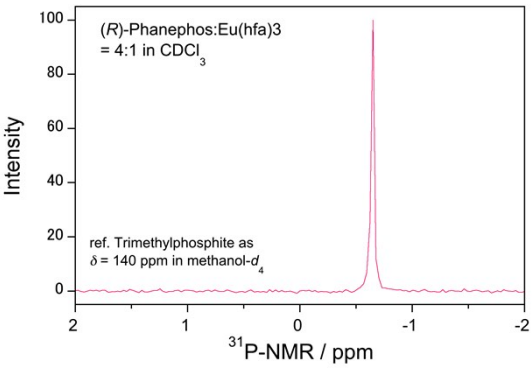

Fig. S6-f. (*R*)-Phanephos : $Eu(hfa)_3$ (4:1).

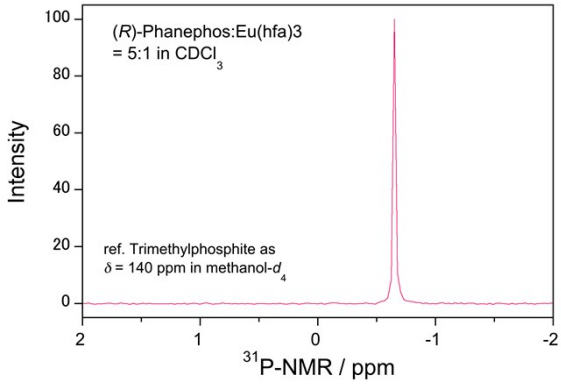

Fig. S6-g. (*R*)-Phanephos : $Eu(hfa)_3$ (5:1).

Fig. S6. ^{31}P-NMR spectra of (*R*)-Phanephos as a function of (*R*)-Phanephos-to-$Eu(hfa)_3$ ratio

in $CDCl_3$.

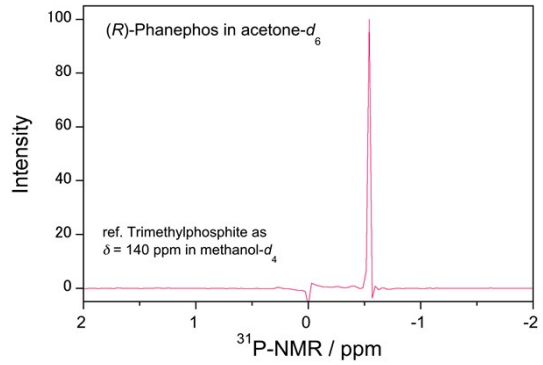

Fig. S7-a. (*R*)-Phanephos : $Eu(hfa)_3$ (1:0).

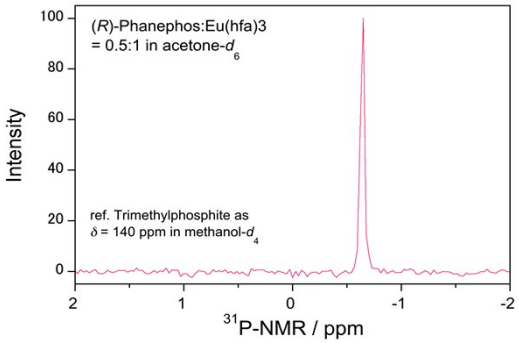

Fig. S7-b. (*R*)-Phanephos : $Eu(hfa)_3$ (0.5:1).

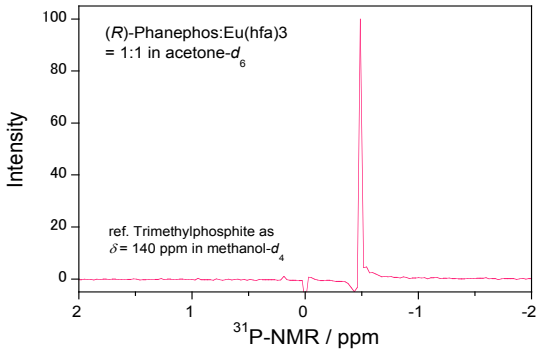

Fig. S7-c. (*R*)-Phanephos : $Eu(hfa)_3$ (1:1).

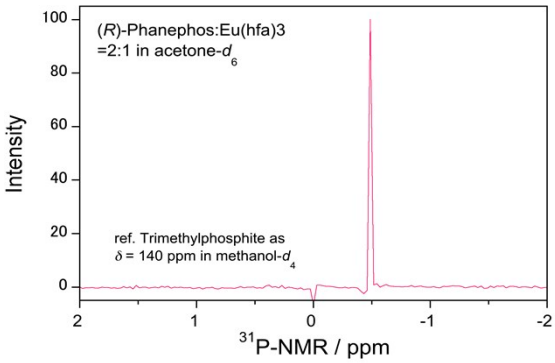

Fig. S7-d. (*R*)-Phanephos : $Eu(hfa)_3$ (2:1).

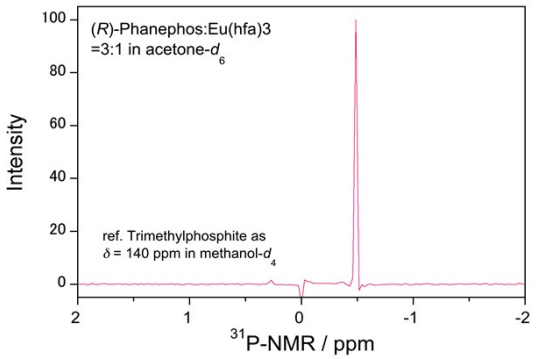

Fig. S7-e. (*R*)-Phanephos : $Eu(hfa)_3$ (3:1).

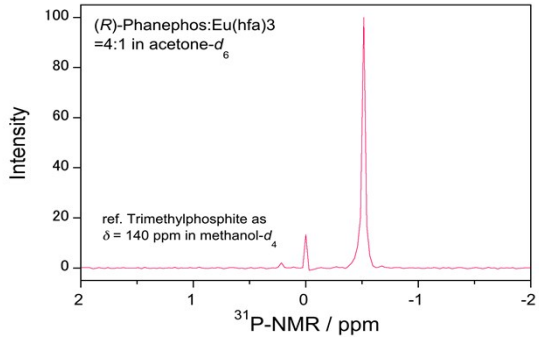

Fig. S7-f. (*R*)-Phanephos : $Eu(hfa)_3$ (4:1).

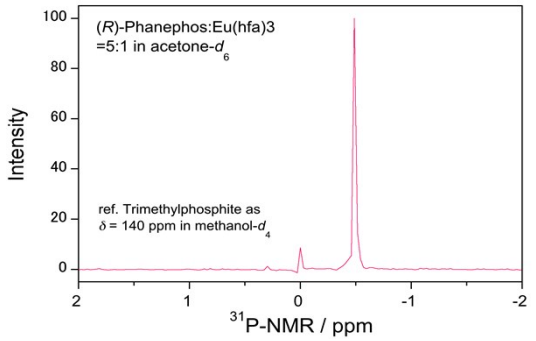

Fig. S7-g. (*R*)-Phanephos : $Eu(hfa)_3$ (5:1).

Fig. S7. ^{31}P-NMR spectra of (*R*)-Phanephos as a function of (*R*)-Phanephos-to-$Eu(hfa)_3$ ratio

in acetone-d_6.

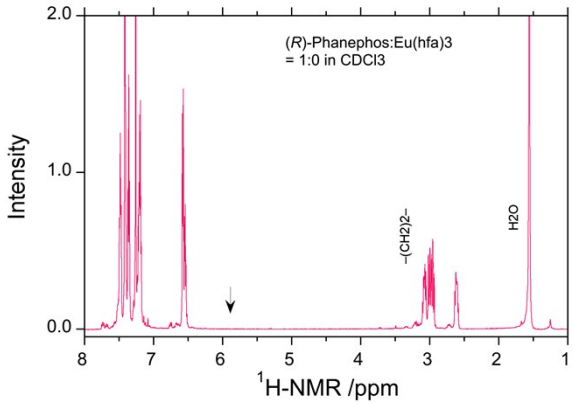

Fig. S8-a. ^{1}H-NMR spectrum of (*R*)-Phanephos without Eu(hfa)$_3$ in $CDCl_3$.

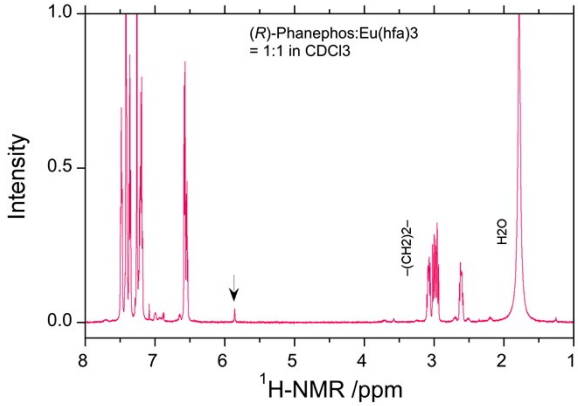

Fig. S8-b. ^{1}H-NMR spectrum of (*R*)-Phanephos with Eu(hfa)$_3$ (1:1) in $CDCl_3$.

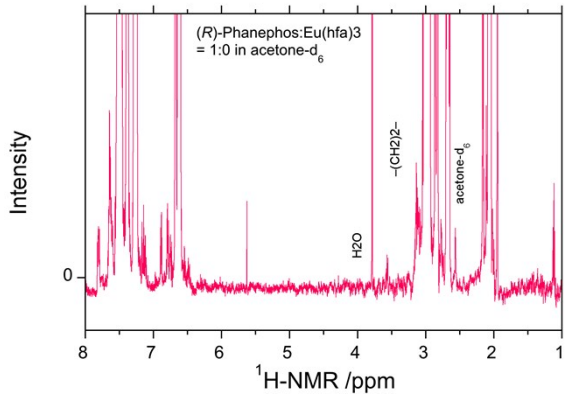

Fig. S9-a. ^{1}H-NMR spectrum of (*R*)-Phanephos without Eu(hfa)$_3$ in acetone-d_6.

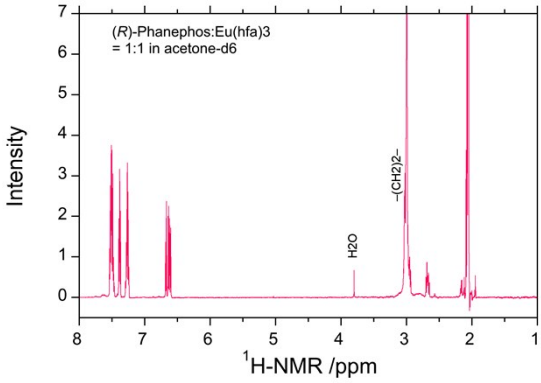

Fig. S9-b. ^{1}H-NMR spectrum of (*R*)-Phanephos with Eu(hfa)$_3$ (1:1) in acetone-d_6.

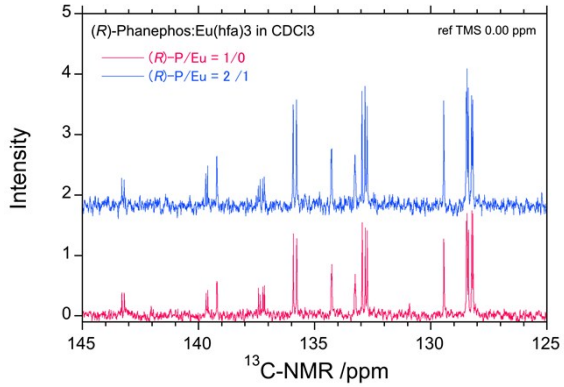

Fig. S10. ^{13}C-NMR spectra of (*R*)-Phanephos with Eu(hfa)$_3$ (1:0 and 2:1) in $CDCl_3$.

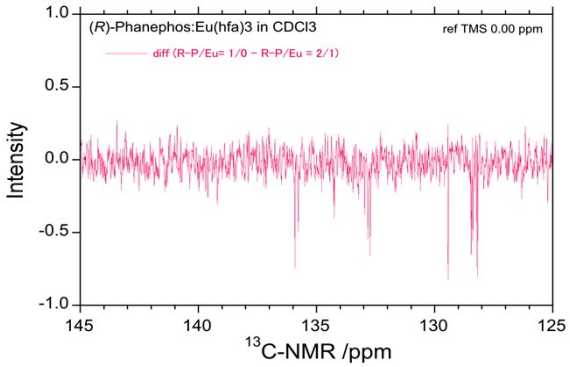

Fig. S11. Difference ^{13}C-NMR spectrum of (*R*)-Phanephos with Eu(hfa)$_3$ (1:0 and 4:1) in $CDCl_3$. Data were taken from **Fig. S10**.

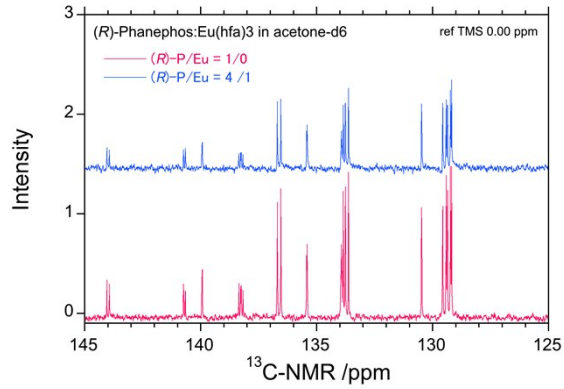

Fig. S12. ^{13}C-NMR spectra of (*R*)-Phanephos with Eu(hfa)$_3$ (1:0 and 4:1) in acetone-d_6.

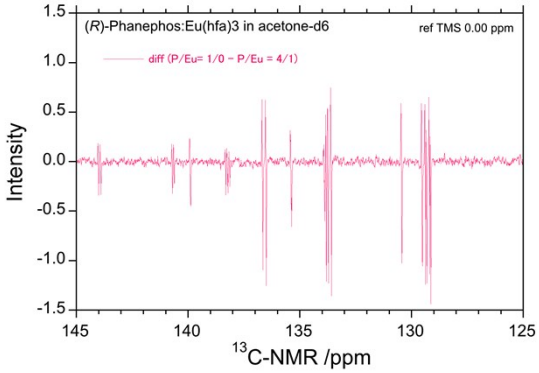

Fig. S13. Difference ^{13}C-NMR spectrum of (*R*)-Phanephos with Eu(hfa)$_3$ (1:0 and 4:1) in acetone-d_6. Data were taken from **Fig. S12**.

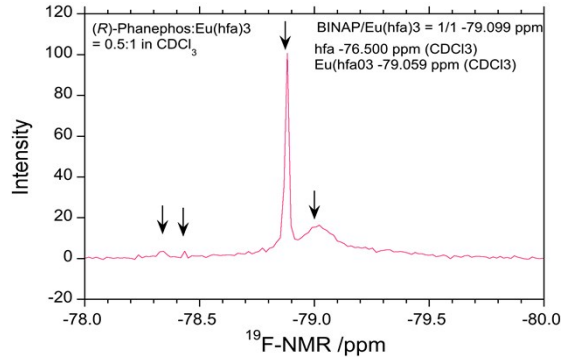

Fig. S14-a. (*R*)-Phanephos and Eu(hfa)$_3$ (0.5:1).

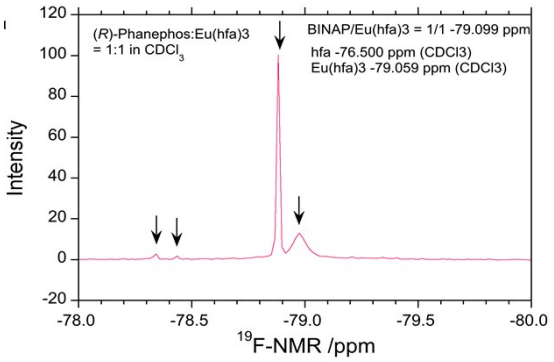

Fig. S14-b. (*R*)-Phanephos and Eu(hfa)$_3$ (1:1).

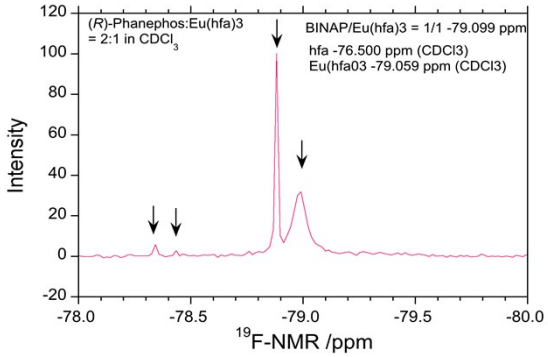

Fig. S14-c. (*R*)-Phanephos and Eu(hfa)$_3$ (2:1).

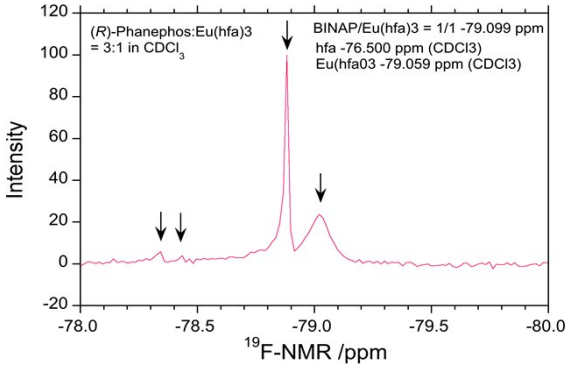

Fig. S14-d. (*R*)-Phanephos and Eu(hfa)$_3$ (3:1).

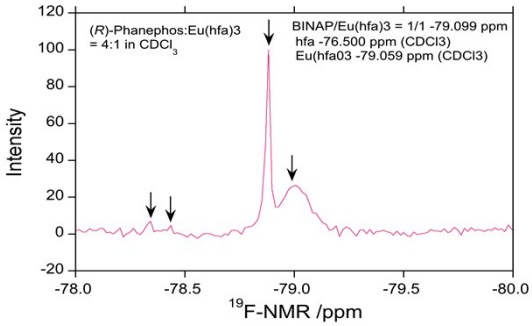

Fig. S14-e. (*R*)-Phanephos and Eu(hfa)$_3$ (4:1).

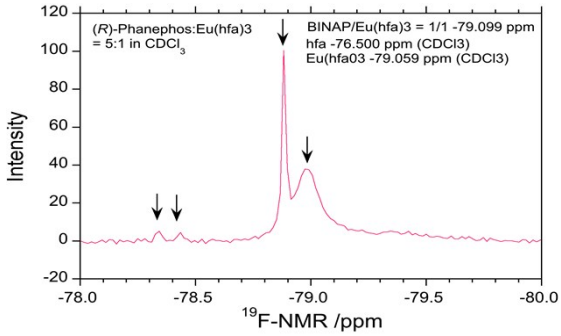

Fig. S14-f. (*R*)-Phanephos and Eu(hfa)$_3$ (5:1).

Fig. S14. ^{19}F-NMR spectra of Eu(hfa)$_3$ as a function of (*R*)-Phanephos-to-Eu(hfa)$_3$ ratio in $CDCl_3$.

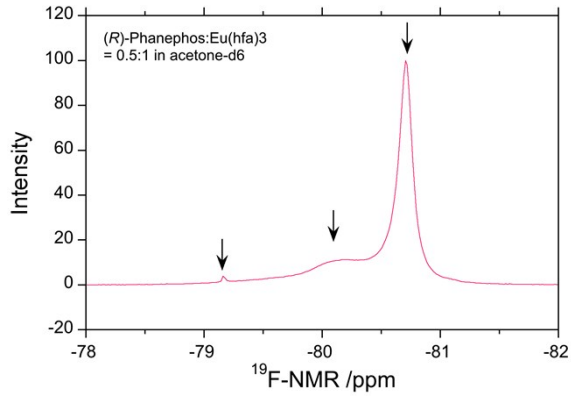

Fig. S15-a. (*R*)-Phanephos and Eu(hfa)$_3$ (0.5:1).

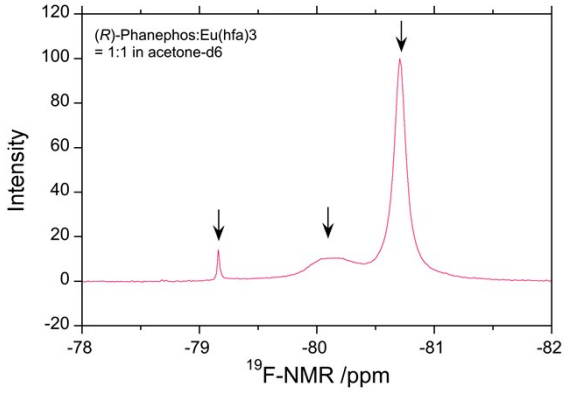

Fig. S15-b. (*R*)-Phanephos and Eu(hfa)$_3$ (1:1).

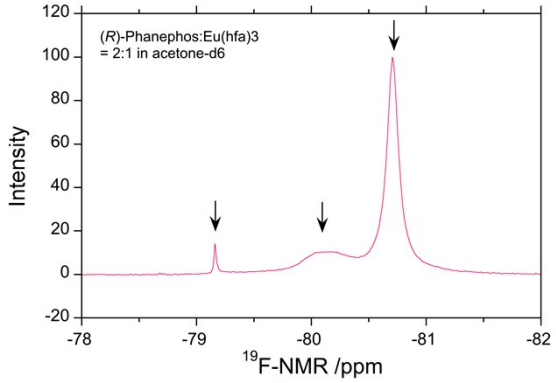

Fig. S15-c. (*R*)-Phanephos and Eu(hfa)$_3$ (2:1).

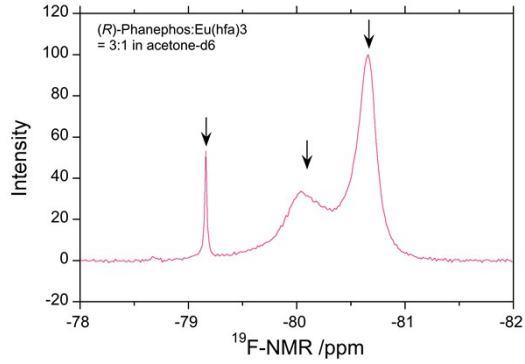

Fig. S15-d. (*R*)-Phanephos and Eu(hfa)$_3$ (3:1).

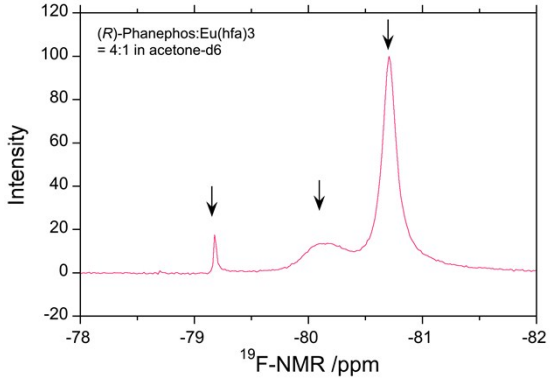

Fig. S15-e. (*R*)-Phanephos and Eu(hfa)$_3$ (4:1).

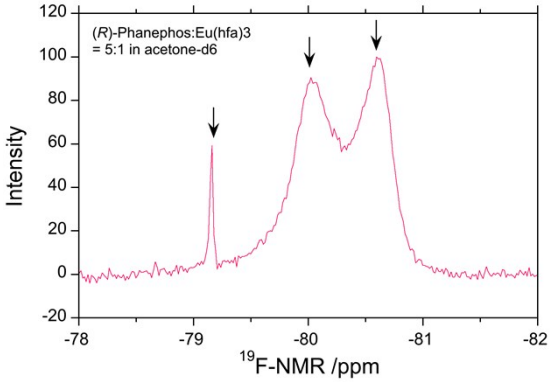

Fig. S15-f. (*R*)-Phanephos and Eu(hfa)$_3$ (5:1).

Fig. S15. ^{19}F-NMR spectra of Eu(hfa)$_3$ as a function of (*R*)-Phanephos-to-Eu(hfa)$_3$ ratio in acetone-d_6.

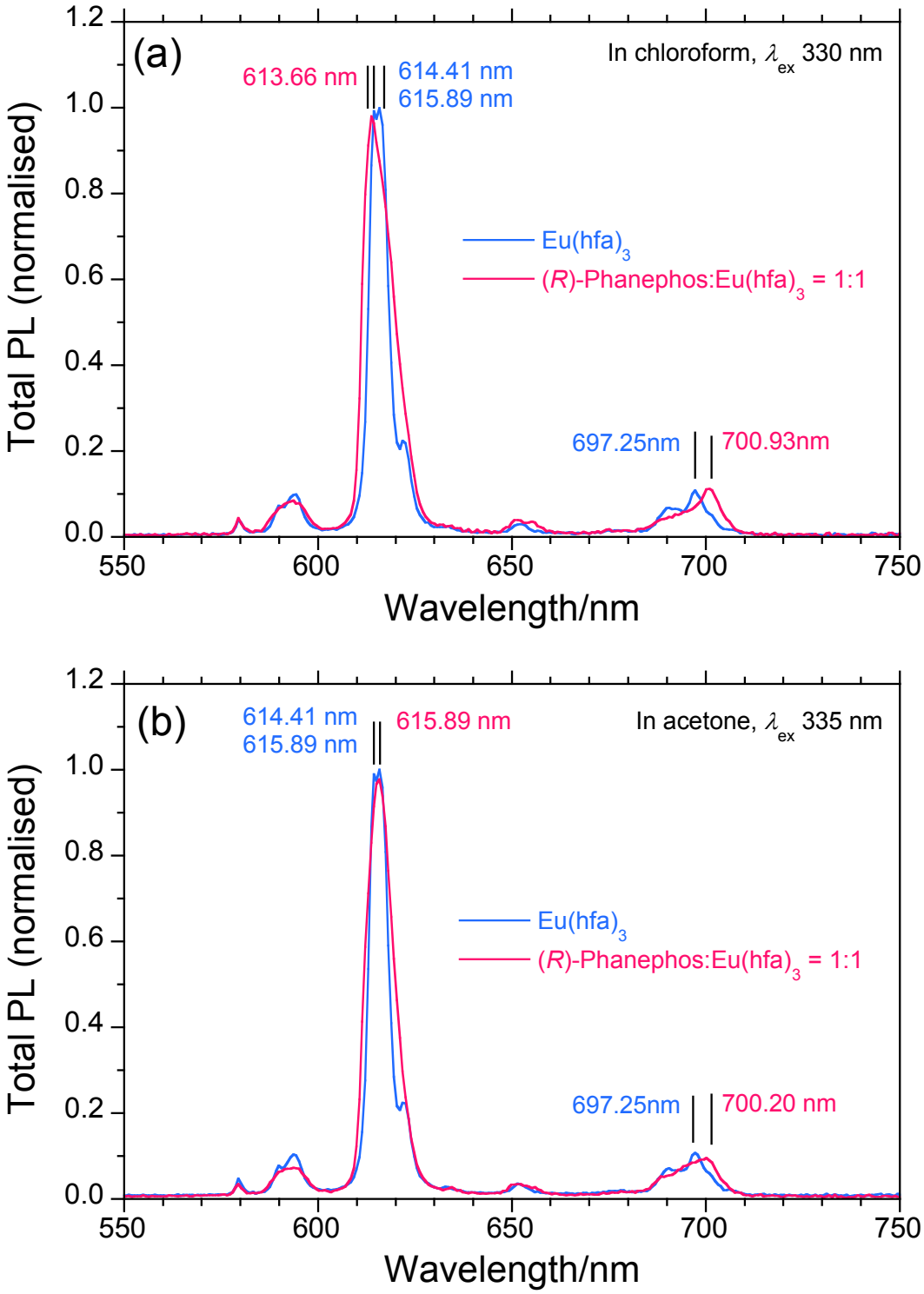

Fig. S16. Comparison of total PL spectra of Eu(hfa)$_3$ with/without an equimolar amount of (*R*)-Phanephos in (a) $CHCl_3$ excited at 330 nm and (b) acetone excited at 335 nm measured with Hamamatsu Photonics with photodiode arrayed detector (C9920-02, spectral resolution 0.75 nm).